HHS Public Access

Author manuscript

Ultrasound Med Biol. Author manuscript; available in PMC 2015 May 12.

Published in final edited form as:

Ultrasound Med Biol. 2015 February ; 41(2): 456–464. doi:10.1016/j.ultrasmedbio.2014.09.033.

TREATMENT OF MICROVASCULAR MICRO-EMBOLIZATION USING MICROBUBBLES AND LONG-TONE-BURST ULTRASOUND: AN *IN VIVO* STUDY

John J. Pacella, **Judith Brands**, **Frederick G. Schnatz**, **John J. Black**, **Xucai Chen**, and **Flordeliza S. Villanueva**

Center for Ultrasound and Molecular Imaging and Therapeutics, University of Pittsburgh School of Medicine, Pittsburgh, Pennsylvania, USA

Abstract

Despite epicardial coronary artery reperfusion by percutaneous coronary intervention, distal micro-embolization into the coronary microcirculation limits myocardial salvage during acute myocardial infarction. Thrombolysis using ultrasound and microbubbles (sonothrombolysis) is an approach that induces microbubble oscillations to cause clot disruption and restore perfusion. We sought to determine whether this technique could restore impaired tissue perfusion caused by thrombotic microvascular obstruction. In 16 rats, an imaging transducer was placed on the biceps femoris muscle, perpendicular to a single-element 1-MHz treatment transducer. Ultrasound contrast perfusion imaging was performed at baseline and after micro-embolization. Therapeutic ultrasound (5000 cycles, pulse repetition frequency = 5 0.33 Hz, 1.5 MPa) was delivered to nine rats for two 10-min sessions during intra-arterial infusion of lipid-encapsulated microbubbles; seven control rats received no ultrasound–microbubble therapy. Ultrasound contrast perfusion imaging was repeated after each treatment or control period, and microvascular volume was measured as peak video intensity. There was a 90% decrease in video intensity after micro-embolization (from 8.6 ± 4.8 to 0.7 ± 0.8 dB, $p < 0.01$). The first and second ultrasound–microbubble sessions were respectively followed by video intensity increases of 5.8 ± 5.1 and 8.7 ± 5.7 dB ($p < 0.01$, compared with micro-embolization). The first and second control sessions, respectively, resulted in no significant increase in video intensity (2.4 ± 2.3 and 3.6 ± 4.9) compared with micro-embolization (0.6 ± 0.7 dB). We have developed an *in vivo* model that simulates the distal thrombotic microvascular obstruction that occurs after primary percutaneous coronary intervention. Long-pulse-length ultrasound with microbubbles has a therapeutic effect on microvascular perfusion and may be a valuable adjunct to reperfusion therapy for acute myocardial infarction.

Keywords

Microvascular obstruction; Ultrasound; Microbubble; Micro-embolization; Sonothrombolysis

Address correspondence to: John J. Pacella, University of Pittsburgh School of Medicine, 200 Lothrop Street, Pittsburgh, PA 15213, USA. pacellajj@upmc.edu.

Conflicts of Interest: There are no relationships with industry to disclose.

INTRODUCTION

Sonothrombolysis capitalizes on unique ultrasound-induced oscillatory behaviors of intravenously injected gas-filled microspheres, or microbubbles, to disrupt intravascular blood clots. Arterial sonothrombolysis studies to date have focused primarily on the dissolution of thrombi that occlude the epicardial coronary or larger cerebral arteries (Birnbaum et al. 1998; Brown et al. 2011; Culp et al. 2011; Kutty et al. 2012; Nishioka et al. 1997; Porter et al. 2001). However, recent pre-clinical data have suggested that the combination of ultrasound and microbubbles can also restore microvascular flow in the setting of AMI or stroke (Culp et al. 2011; Nedelmann et al. 2010; Porter 2009; Xie et al. 2009), raising the possibility that sonothrombolysis might be an effective strategy for treating the component of post-ischemic microvascular hypoperfusion caused by distal micro-embolization of atherothrombotic debris. We recently developed an *in vitro* model of microvascular thrombo-embolism and illustrated the efficacy of sonothrombolysis using long-tone-burst, high-acoustic-pressure ultrasound (Leeman et al. 2012). In the present study, we tested the hypothesis that insonification of microbubbles with long-tone-burst ultrasound is an effective treatment for microvascular thrombo-embolism *in vivo*. We recapitulated clinical thrombotic micro-embolization by embolizing microthrombi into the distal microcirculation of the rat hindlimb. We then treated the hindlimb microvasculature with ultrasound and microbubbles, using the ultrasound parameters that were found to be effective in our *in vitro* study, and used contrast ultrasound to measure perfusion.

METHODS

Preparation of microthrombi

Micron-sized thrombi were prepared by mixing 1.5 mL citrated venous porcine blood (Lampire Biological Labs, Ottsville, PA, USA) with 0.25 M $CaCl_2$ solution (150 μL) in a 2.5-mL glass vial and then incubating at room temperature for 3 h (Leeman et al. 2012; Nishioka et al. 1997). The glass vial was then shaken in a dental amalgamator for 1–2 s to fragment the clot. To achieve thrombi smaller than 200 μm, the thrombus-containing suspension was passed five times at each step through a series of progressively narrower needles (18 gauge down to 27 gauge), then subsequently passed through a 200-μm-pore mesh. Size distribution of the microthrombi was measured using Multisizer 3 Coulter Counter (Beckman Coulter, Pasadena, CA, USA).

Microbubble preparation

Perfluorobutane-filled, lipid-encapsulated microbubbles were prepared for the sonothrombolysis treatment as previously described (Weller et al. 2002). Briefly, a mixture of 1,2-distearoyl-sn-glycero-3-phosphocholine (4 mg/mL), 1,2-distearoyl-*sn*-glycero-3-phosphoethanolamine (2 mg/mL) and polyethylene glycol (2 mg/mL) was sonicated using a probe-type apparatus at a power setting of 5 (XL2020, Misonix, Farmingdale, NY, USA) for a total duration of 1.5 min in the presence of perfluorobutane gas to produce microbubbles with a mean diameter of 3 μm and a concentration of $1–2 \times 10^9$ microbubbles/mL. Contrast

perfusion imaging was performed using Definity (1.2×10^{10} microbubbles/mL, Perflutren Lipid Microsphere, Lantheus Medical Imaging, North Billerica, MA, USA).

Animal preparation

All experimental protocols were approved by the Institutional Animal Care and Use Committee of the University of Pittsburgh. Young Wistar male rats (n = 16) weighing 263 ± 22 g were anesthetized with isoflurane (3%) and maintained with 2% isoflurane. The right external jugular vein was cannulated with a 20G angiocatheter for infusion of Definity for perfusion imaging. Polyethylene tubing (PE-10, Becton Dickinson, Franklin Lakes, NJ, USA) was advanced from the right femoral artery into the abdominal aorta for administration of microthrombi into the left hindlimb and subsequent therapeutic microbubble infusion. The left hindlimb was degloved to allow direct visualization of the hindlimb muscle for positioning of the ultrasound transducers. Heart rate, respiratory rate and oxygen saturation were monitored continuously using a small animal vital signs monitor (MouseOx, Starr Life Science, Holliston, MA, USA). Figure 1 is a photograph of our experimental setup.

Ultrasound imaging and therapy

A clinical ultrasound imaging system (Sequoia 512, Siemens: Mountain View, CA, USA) was used to measure hindlimb muscle perfusion using a contrast-specific mode combining phase and amplitude modulation (Phillips 2001) of ultrasound signals from a linear array transducer (15L8, Siemens., 7 MHz: Mountain View, CA, USA). With the rat in the right lateral decubitus position, the transducer was positioned anterior to the muscle, and imaging proceeded in the longitudinal plane along the muscle's midsection. Burst-replenishment imaging was performed during continuous intravenous infusion of Definity at 1–2 mL/h (mechanical index 5 1.9 for burst and 0.2 for replenishment imaging) (Villanueva et al. 2001; Wei et al. 1998).

Therapeutic ultrasound was delivered with a flat single-element immersion transducer 12.7 mm in diameter (A303S, Olympus NDT, Center Valley, PA, USA), driven by an arbitrary function generator (AFG3252, Tektronix, Aliquippa, PA, USA) connected to a gated radio-frequency power amplifier (Model 250A250AM8, Amplifier Research, Bothell, WA, USA). The therapy transducer was oriented directly over the lateral aspect of the biceps femoris, orthogonal to the imaging transducer, such that the muscle was in the near field of the transducer and within the treatment area, as confirmed by visualizing microbubble destruction in the perfusion image immediately after delivery of a therapeutic pulse. Therapy ultrasound was delivered at 1 MHz, 1.5 MPa, 5000 cycles and 3-s pulse interval (duty cycle 0.167%) for each of two 10-min sessions. The ultrasound field was calibrated with a 200-μm capsule hydrophone (HGL-0200, Onda, Sunnyvale, CA, USA). The −6-dB beam width was 5.0 mm. The spatial peak-temporal average intensity (I_{SPTA}) was 0.125 W/cm^2. The spatial average-temporal average intensity (I_{SATA}) in the cylindrical volume in front and over the footprint of the therapy transducer was 0.031 W/cm^2.

Experimental protocol

Baseline time-triggered ultrasound contrast perfusion imaging of the hindlimb was performed. Next, 0.25- to 0.5-mL increments of microthrombus suspension were injected into the arterial line until perfusion was reduced by at least 50% (defined as a reduction in peak plateau video intensity by visual assessment of the contrast ultrasound images). After a 10-min waiting period, perfusion imaging was repeated to confirm persistent hindlimb hypoperfusion. If perfusion improved to >50% of baseline, additional microthrombi were given, followed by perfusion imaging 10 min later; this sequence was repeated until persistent (10 min) hypoperfusion was attained. Then, treatment microbubbles were delivered (3 mL/h) over 10 min into the hindlimb during simultaneous ultrasound delivery using the acoustic regimen outlined above. Ultrasound perfusion imaging with intravenous microbubble infusion was then performed, followed by another 10-min treatment session and repeat perfusion imaging (n = 9). In control rats (n = 7), neither ultrasound nor treatment microbubbles were given after micro-embolization, but perfusion imaging was performed at the same time points as in the treatment group. At the end of the experiment, animals were euthanized using isoflurane (5%).

Image analysis

Digitally acquired ultrasound perfusion movies encompassing the initial post-destruction image (background) up to and including the peak plateau video intensity frames (full microbubble replenishment) were analyzed using image processing software (MATLAB, The MathWorks, Natick, MA, USA). For each movie, the frames were averaged to generate a single frame (Fig. 2) to guide drawing of a region of interest (ROI) encompassing either the entire hindlimb muscle (both micro- and macrovasculature) (Fig. 2, *red*) or solely the microvasculature (Fig. 2, *yellow*). Average pixel video intensity (dB) was measured in the region of interest for each frame of the movie, and video intensity (*y*)-versus-time (*t*) data were fit to a mono-exponential curve as previously described (Wei et al. 1998):

$$y(t) = A \times \left(1 - e^{-\beta t}\right),$$

where ß reflects microbubble (red blood cell) velocity, and *A* is the peak plateau video intensity, which reflects vascular cross-sectional area. Because micro-embolization would cause microvascular obstruction, it would be expected to reduce cross-sectional area. Thus, the *A* term was used to track responses to micro-embolization and to ultrasound–microbubble treatment. Histology of hindlimb muscle was performed *post mortem* in both treatment and control animals to determine whether ultrasound–microbubble therapy was associated with less thrombotic microvascular obstruction. Fixed samples were stained with hematoxylin and eosin, and the sections were examined microscopically.

Statistics

Data are expressed as the mean ± standard deviation. Differences among vascular cross-sectional measurements derived from the video intensity–time curves (A) at the different experimental stages were assessed using repeated-measures analysis of variance. When a difference was detected (analysis of variance, $p < 0.05$), a Bonferroni *post hoc t*-test was

performed, where significance was defined at $p < 0.0125$, to adjust for multiple comparisons.

RESULTS

Microthrombi

Thrombus particle size varied from 10 to 200 μm. Mean diameter was 17.3 ± 3.0 μm, and the concentration of the suspension was $2.1 \pm 0.4 \times 10^5$ thrombi/mL. A representative size distribution of a microthrombus suspension is illustrated in Figure 3.

Contrast perfusion imaging

In Figure 4 are peak plateau video intensity still frame contrast ultrasound images from both a representative control (top) and treatment (bottom) animal for each experimental stage (baseline, micro-embolization, therapy 1 [or control] and therapy 2 [or control]). In the control animal, there was a marked decrease in perfusion after micro-embolization that persisted throughout both control periods. In the treatment animal, there was a pronounced improvement in video intensity after both therapy 1 and therapy 2.

Microvascular blood volume

There was a significant difference among the experimental stages with respect to the peak plateau video intensity (A), our index of microvascular cross-sectional area, measured from the microvascular ROI (analysis of variance, $p < 0.05$). The A term significantly decreased from baseline after micro-embolization in the treatment animals (from 8.6 ± 4.8 to 0.7 ± 0.8 dB, $p < 0.01$) and controls (from 10.7 ± 5.3 to 0.6 ± 0.7 dB, $p < 0.01$) (Fig. 5). After 10 min of ultrasound–microbubble treatment, there was a strong trend ($p = 0.015$) toward an increase in A compared with the micro-embolization stage (to 5.8 ± 5.1 dB), and *A* was no longer significantly different from pre-embolization baseline. After 10 additional min of therapy, perfusion improved further, such that A was significantly higher than that after micro-embolization (0.7 ± 0.8 to 8.7 ± 5.7 dB, $p < 0.01$). In control rats, after 10 min without treatment, *A* was numerically higher than, but not statistically different from that measured after micro-embolization (2.4 ± 2.3 dB). After an additional 10 min without therapy, A remained significantly lower (3.6 ± 4.9 dB) than baseline.

Total blood volume

When both the microcirculation and the larger feeding vessels constituting the macrovasculature were included in the ROI, there was a significant reduction in *A* ($p < 0.01$) after micro-embolization in both the treatment (10.9 ± 4.0 to 1.9 ± 2.0 dB, $p < 0.01$) and control (12.1 ± 5.1 to 2.8 ± 3.5 dB, $p < 0.01$, Fig. 6) rats, compared with baseline. After the first ultrasound–microbubble therapy session, A returned toward baseline (9.1 ± 5.6 dB, $p < 0.01$), and remained so after the second therapy (9.1 ± 5.3 dB). In the control animals, A remained significantly lower than baseline and remained unchanged compared with micro-embolization for both 10-min sessions without treatment (3.6 ± 3.0 and 4.3 ± 5.0 dB).

In Figure 7 are images of representative hematoxylin and eosin-stained sections from four micro-embolized rats, two of which received ultrasound treatment (bottom panels) and two

of which received no therapy (top panels). Whereas the untreated animals had multiple occluded microvessels, the microvessels in the treated rats were patent. These observations were consistent with the results in the contrast perfusion images. Additionally, as illustrated in Figure 7, there was no evidence of microvessel trauma, hemorrhage or architectural derangements directly under the therapeutic single-element transducer: the tissue is qualitatively indistinguishable from control skeletal muscle. Further, we did not observe any gross evidence of hemorrhage on visual inspection of the tissue after therapy.

DISCUSSION AND CONCLUSIONS

In this study, we found that microbubble delivery in the presence of site-directed ultrasound restored microvascular perfusion in a rat hindlimb model of micro-embolization. Specifically, ultrasound parameters incorporating high acoustic pressures and long cycle length, which are known to induce microbubble inertial cavitation, significantly improved microvascular perfusion to the embolized bed. In our previous *in vitro* studies, we found that this same ultrasound regime results in microclot dissolution; we thus infer that the ultrasound microbubble intervention facilitated disruption of the embolized fragments in the present study. As such, this is a novel technique for treating the component of microvascular obstruction caused by micro-embolization in the setting of percutaneous interventions for coronary artery disease.

Micro-embolization during coronary interventions

Micro-embolization is highly prevalent during angioplasty and stenting (Herrmann 2005; Heusch et al. 2009; Topol and Yadav 2000). The use of Doppler monitoring during carotid stenting procedures revealed that virtually every patient had evidence of micro-embolization of upstream plaque components (Jordan et al. 1999). Herrmann and co-workers (Herrmann 2005) observed periprocedural myocardial injury—to a large extent caused by mobilization of plaque debris, thrombi and microparticles—in about 25% of all coronary PCI procedures. The untoward effects of this phenomenon on microvascular perfusion provide a therapeutic target for improving the outcomes of patients undergoing PCI.

In the present study, we focused on the thrombotic component of microvascular obstruction, and did not include cholesterol crystals and other plaque components, which also likely play a role in poor microvascular perfusion post-PCI. However, microthrombotic occlusion plays an important role in micro-embolization, as autopsy studies have reported that nearly 50% of microvascular occlusion is caused by microthrombi (Saber et al. 1993). Therefore, our model of microvascular micro-embolization is a clinically relevant experimental system for evaluating treatment strategies to treat the microvascular hypoperfusion observed in many patients undergoing PCI for acute myocardial infarction.

Effects of ultrasound–microbubble interactions

That appropriately tuned ultrasound can cause the compression and expansion, or even destruction, of microbubbles has long been known (Leighton 1994). Such microbubble acoustic behaviors are the basis for the detection strategies employed in current ultrasound systems for imaging ultrasound contrast agents in diagnostic echocardiography (Mulvagh et

al. 2000). More recently, however, it has become evident that the unique acoustic behaviors of microbubbles can also be harnessed for therapeutic gain (Ferrara et al. 2007) in a variety of medical conditions, including thrombotic vessel occlusion, in which ultrasound-induced microbubble vibrations are used to disrupt blood clots.

The mechanism underlying microbubble-mediated clot disruption is incompletely understood. It has been hypothesized that ultrasound-induced stable and/or inertial cavitation play a significant role (Liu and Wu 2009; Postema et al. 2004). Cyclic microbubble vibrations (stable cavitation) may result in the formation of streamlines and shear stress around the microbubble (Liu and Wu 2009), which may mechanically disrupt nearby clots and/or further mix endogenous tissue plasminogen activator into the thrombus to allow further dissolution (Datta et al. 2008). Non-linear microbubble expansions and, eventually, violent microbubble collapse at higher acoustic pressures (inertial cavitation) can cause microjetting (Postema et al. 2004) and formation of non-encapsulated, secondary microbubbles. Microjets may erode the clot surface to cause disruption of clot integrity, and secondary bubbles may themselves oscillate and create more jets (Chen et al. 2014). Our own group has previously reported that microbubbles flowing past a thrombus in the presence of inertial cavitation ultrasound regime cause clot pitting *in vitro* (Kim et al. 2012). Further, using ultra-high-speed imaging (Chen et al. 2013), we have recently observed *in vitro* that inertial cavitation behavior of microbubbles adjacent to a clot alternately invaginates and stretches the thrombus, ultimately leaving indentations in the thrombus after microbubble destruction (Chen et al. 2014).

Other *in vitro* studies have observed the efficacy of ultrasound-assisted thrombolysis, with and without recombinant tissue plasminogen activator, in the presence of microbubbles, and have suggested that cavitation-related phenomena are responsible for this effect (Brown et al. 2011; Datta et al. 2006; Porter et al. 1996, 2001). Several *in vivo* studies in animal models with thrombus occluding a major feeding artery have found that ultrasound and microbubble treatment restores flow to ischemic regions (Birnbaum et al. 1998; Brown et al. 2011; Culp et al. 2011; Kutty et al. 2012; Nishioka et al. 1997; Porter et al. 2001). This was reported in rabbit and pig models in the iliofemoral artery, internal carotid artery, left circumflex coronary artery and superior vena cava, using inertial (Birnbaum et al. 1998; Kutty et al. 2012; Nishioka et al. 1997; Porter et al. 2001) as well as stable (Brown et al. 2011; Culp et al. 2011; Porter et al. 2001) cavitation regimes. In contrast to the present work, these studies have focused on large vessel thrombi. An important distinction of our study is that we specifically evaluated the effect of microbubble–ultrasound-mediated clot disruption within the microcirculation—an area that is often overlooked during reperfusion therapy—and, for the first time, proved that ultrasound–microbubble interactions can mitigate microvascular obstruction caused by embolization of microthrombi.

Other potential mechanisms include endothelial nitric oxide release by ultrasound, which has been previously described at low ultrasound frequency (27 kHz) (Siegel et al. 2004; Suchkova et al. 2002), without microbubbles; it is unclear if this phenomenon occurred in our study, which used higher ultrasound frequencies and microbubbles. This observation requires confirmation in more studies, and the role of nitric oxide release in ultrasound–microbubble-mediated reperfusion needs to be determined. In this regard, it is possible that

nitric oxide causes vasodilation and further dislodgement of microthombi, platelet inhibition and decreased expression of endothelial inflammatory adhesion molecules, all of which could contribute therapeutically to myocardial salvage.

Acoustic requirements for microvascular sonothrombolysis

Disruption of the microvascular microthrombi implicated in myocardial micro-embolization likely requires ultrasound parameters (*e.g.*, pulse length, acoustic pressure) different from those used in larger vessels as the underlying physiology, architecture and fluid dynamics of the microcirculation are different. To define the optimal acoustic regimen to achieve microvascular sonothrombolysis, we recently reported a novel *in vitro* flow system that simulates microvascular embolization such as occurs after PCI and sought to determine effective ultrasound parameters for clot disruption (Leeman et al. 2012). We found that thrombus burden was most effectively reduced when ultrasound was delivered to the microbubbles at acoustic pressures above the threshold for inertial cavitation, and that longer pulses, that is, ≥1000 cycles, further augmented efficacy. In the present study, these *in vitro* data informed the selection of ultrasound parameters: we chose to expose microbubbles to a high acoustic pressure and long pulse duration and improved perfusion after microvascular embolization *in vivo*, as occurred in our *in vitro* studies.

Limitations

There are several limitations to our study. To our knowledge, this is the first report of an animal model that specifically simulates the thrombotic micro-embolization component of microvascular obstruction. Although this model allowed us to specifically test the effect of ultrasound microbubble interactions on thromboembolic occlusion of the microcirculation, it does not fully recapitulate the multifaceted post-ischemic no-reflow scenario as originally described by Kloner et al. (1974), nor does it fully encompass all features of no reflow in the contemporary PCI era, in that our micro-emboli were not composed of other plaque components that typically embolize along with thrombi. Further, our model was not developed on a background of longstanding vascular disease that would exist clinically; thus, attributes that could affect sonothrombolytic efficacy, such as microvascular endothelial dysfunction, did not co-exist with the micro-embolization. Nonetheless, our study provides the first proof of concept that microvascular hypoperfusion resulting from thrombotic micro-embolism can be alleviated with ultrasound and microbubble therapy. Future studies incorporating a more fully representative pathophysiologic background for the clinical no-reflow phenomenon after PCI will be an important next step to further develop this treatment strategy.

Another limitation is the short duration/acute nature of these studies. Maintenance of the therapeutic effect on perfusion beyond the time studied in our experiments would be important for clinical translation. Future studies in both rodents and pigs will be performed to test the lasting efficacy of this therapy. Additionally, we used only contrast-enhanced ultrasound to measure the therapeutic effect. Other measures, such as pH and venous lactate, could provide additional corroborative physiologic measures of therapeutic success.

When acoustic pressure is above the threshold for inertial cavitation such as in the present study, microbubbles are likely to be destroyed within a few cycles of ultrasound exposure. However, our previous *in vitro* data indicated that prolonged pulse lengths, above the minimum number of cycles adequate to cause cavitation of the encapsulated microbubbles, are actually required to cause clot disruption (Leeman et al. 2012); the mechanisms underlying this requirement remain unclear. Also, only a relatively high acoustic pressure typical of inertial cavitation was applied in the present study. The contribution of lower acoustic pressures typical of stable cavitation to treatment efficacy in an *in vivo* model has yet to be studied. Further, whereas mechanical and fluid dynamic effects of microbubble oscillation have been posited to underlie the efficacy of this treatment paradigm, other potential biological effects of microbubble acoustic behavior that facilitate microvascular reperfusion, including vasodilation, remain to be explored.

Finally, we did not use antiplatelet, anticoagulant or thrombolytic agents in this study. Other groups have reported successful large vessel sonothrombolysis with and without these agents (Birnbaum et al. 1998; Brown et al. 2011; Culp et al. 2011; Kutty et al. 2012; Nishioka et al. 1997; Porter et al. 2001; Xie et al. 2009). As we were primarily interested in isolating the effects of ultrasound and microbubbles, anticoagulant or antiplatelet agents were not administered.

Clinical implications

Embolization of thrombotic plaque components to the distal microvasculature during PCI is a prevalent phenomenon that leads to suboptimal microvascular perfusion despite apparent patency of the epicardial coronary artery. This phenomenon is associated with higher morbidity, and treatment strategies are currently suboptimal. Our data suggest that microbubbles and ultrasound applied specifically to the microcirculation may be a new approach to enhance microvascular perfusion, as an adjunctive therapy immediately after PCI of the upstream epicardial coronary artery. Before any clinical application, however, systematic analysis and determination of the most tolerable and optimal acoustic parameters for achieving microvascular reperfusion would be required. Nonetheless, as indicated in our study, the capacity to simultaneously image perfusion during therapeutic microbubble infusion confers the additional possibility for immediate real-time feedback on the response to treatment. These dual capabilities render this theranostic technology a potentially powerful noninvasive, bedside, non-pharmacologic approach for attenuating microvascular obstruction in patients undergoing PCI.

Acknowledgments

The authors thank Linda Lavery and Regeant Panday for their valuable technical assistance. F. S. Villanueva is supported in part by the National Institutes of Health (R01EB016516, R21CA167373). J. J. Pacella is supported in part by Pittsburgh Foundation Grant.

References

Birnbaum Y, Luo H, Nagai T, Fishbein MC, Peterson TM, Li SP, Kricsfeld D, Porter TR, Siegel RJ. Noninvasive in vivo clot dissolution without a thrombolytic drug: Recanalization of thrombosed iliofemoral arteries by transcutaneous ultrasound combined with intravenous infusion of microbubbles. Circulation. 1998; 97:130–134. [PubMed: 9445162]

Brown AT, Flores R, Hamilton E, Roberson PK, Borrelli MJ, Culp WC. Microbubbles improve sonothrombolysis in vitro and decrease hemorrhage in vivo in a rabbit stroke model. Investigative Radiology. 2011; 46:202–207. [PubMed: 21150788]

Chen X, Leeman JE, Wang J, Pacella JJ, Villanueva FS. New insights into mechanisms of sonothrombolysis using ultra high speed imaging. Ultrasound Med Biol. 2014; 40:258–262. [PubMed: 24139920]

Chen X, Wang J, Versluis M, de Jong N, Villanueva FS. Ultra-fast bright field and fluorescence imaging of the dynamics of micrometer-sized objects. Rev Sci Instrum. 2013; 84:063701. [PubMed: 23822346]

Culp WC, Flores R, Brown AT, Lowery JD, Roberson PK, Hennings LJ, Woods SD, Hatton JH, Culp BC, Skinner RD, Borrelli MJ. Successful microbubble sonothrombolysis without tissue-type plasminogen activator in a rabbit model of acute ischemic stroke. Stroke. 2011; 42:2280–2285. [PubMed: 21700942]

Datta S, Coussios CC, Ammi AY, Mast TD, de Courten-Myers GM, Holland CK. Ultrasound-enhanced thrombolysis using Definity as a cavitation nucleation agent. Ultrasound Med Biol. 2008; 34:1421–1433. [PubMed: 18378380]

Datta S, Coussios CC, McAdory LE, Tan J, Porter T, De Courten-Myers G, Holland CK. Correlation of cavitation with ultrasound enhancement of thrombolysis. Ultrasound Med Biol. 2006; 32:1257–1267. [PubMed: 16875959]

Ferrara K, Pollard R, Borden M. Ultrasound microbubble contrast agents: Fundamentals and application to gene and drug delivery. Annu Rev Biomed Eng. 2007; 9:415–447. [PubMed: 17651012]

Go AS, Mozaffarian D, Roger VL, Benjamin EJ, Berry JD, Borden WB, Bravata DM, Dai S, Ford ES, Fox CS, Franco S, Fullerton HJ, Gillespie C, Hailpern SM, Heit JA, Howard VJ, Huffman MD, Kissela BM, Kittner SJ, Lackland DT, Lichtman JH, Lisabeth LD, Magid D, Marcus GM, Marelli A, Matchar DB, McGuire DK, Mohler ER, Moy CS, Mussolino ME, Nichol G, Paynter NP, Schreiner PJ, Sorlie PD, Stein J, Turan TN, Virani SS, Wong ND, Woo D, Turner MB. Executive summary: Heart disease and stroke statistics—2013 update: A report from the American Heart Association. Circulation. 2013; 127:143–152. [PubMed: 23283859]

Goldstein JA, Maini B, Dixon SR, Brilakis ES, Grines CL, Rizik DG, Powers ER, Steinberg DH, Shunk KA, Weisz G, Moreno PR, Kini A, Sharma SK, Hendricks MJ, Sum ST, Madden SP, Muller JE, Stone GW, Kern MJ. Detection of lipid-core plaques by intracoronary near-infrared spectroscopy identifies high risk of periprocedural myocardial infarction. Circ Cardiovasc Interv. 2011; 4:429–437. [PubMed: 21972399]

Herrmann J. Peri-procedural myocardial injury: 2005 update. Eur Heart J. 2005; 26:2493–2519. [PubMed: 16176941]

Heusch G, Kleinbongard P, Bose D, Levkau B, Haude M, Schulz R, Erbel R. Coronary microembolization: From bedside to bench and back to bedside. Circulation. 2009; 120:1822–1836. [PubMed: 19884481]

Isshiki T, Kozuma K, Kyono H, Suzuki N, Yokoyama N, Yamamoto Y. Initial clinical experience with distal embolic protection using “Fil-trap,” a novel filter device with a self-expandable spiral basket in patients undergoing percutaneous coronary intervention. Cardiovasc Interv Ther. 2010; 26:12–17. [PubMed: 24122493]

Ito H, Maruyama A, Iwakura K, Takiuchi S, Masuyama T, Hori M, Higashino Y, Fujii K, Minamino T. Clinical implications of the ‘no reflow’ phenomenon: A predictor of complications and left ventricular remodeling in reperfused anterior wall myocardial infarction. Circulation. 1996; 93:223–228. [PubMed: 8548892]

Ito H, Tomooka T, Sakai N, Yu H, Higashino Y, Fujii K, Masuyama T, Kitabatake A, Minamino T. Lack of myocardial perfusion immediately after successful thrombolysis: A predictor of poor recovery of left ventricular function in anterior myocardial infarction. Circulation. 1992; 85:1699–1705. [PubMed: 1572028]

Jordan WD Jr, Voellinger DC, Doblar DD, Plyushcheva NP, Fisher WS, McDowell HA. Microemboli detected by transcranial Doppler monitoring in patients during carotid angioplasty versus carotid endarterectomy. Cardiovasc Surg. 1999; 7:33–38. [PubMed: 10073757]

Kaul S. Sonothrombolysis: A universally applicable and better way to treat acute myocardial infarction and stroke? Who is going to fund the research? Circulation. 2009; 119:1358–1360. [PubMed: 19255337]

Kim JS, Leeman JE, Kagemann L, Yu FT, Chen X, Pacella JJ, Schuman JS, Villanueva FS, Kim K. Volumetric quantification of in vitro sonothrombolysis with microbubbles using high-resolution optical coherence tomography. J Biomed Opt. 2012; 17:070502. [PubMed: 22894458]

Kloner RA, Ganote CE, Jennings RB. The “no-reflow” phenomenon after temporary coronary occlusion in the dog. J Clin Invest. 1974; 54:1496–1508. [PubMed: 4140198]

Kutty S, Wu J, Hammel JM, Xie F, Gao S, Drvol LK, Lof J, Radio SJ, Therrien SL, Danford DA, Porter TR. Microbubble mediated thrombus dissolution with diagnostic ultrasound for the treatment of chronic venous thrombi. PLoS ONE. 2012; 7:e51453. [PubMed: 23251539]

Leeman JE, Kim JS, Yu FT, Chen X, Kim K, Wang J, Chen X, Villanueva FS, Pacella JJ. Effect of acoustic conditions on microbubble-mediated micro-vascular sonothrombolysis. Ultrasound Med Biol. 2012; 38:1589–1598. [PubMed: 22766112]

Leighton, T. The acoustic bubble. San Diego: Academic Press; 1994.

Lincoff AM, Topol EJ. Illusion of reperfusion. Does anyone achieve optimal reperfusion during acute myocardial infarction? Circulation. 1993; 88:1361–1374. [PubMed: 8353902]

Liu X, Wu J. Acoustic microstreaming around an isolated encapsulated microbubble. J Acoust Soc Am. 2009; 125:1319–1330. [PubMed: 19275289]

Montorsi P, Caputi L, Galli S, Ciceri E, Ballerini G, Agrifoglio M, Ravagnani P, Trabattoni D, Pontone G, Fabbiocchi F, Loaldi A, Parati E, Andreini D, Veglia F, Bartorelli AL. Microembolization during carotid artery stenting in patients with high-risk, lipid-rich plaque: A randomized trial of proximal versus distal cerebral protection. J Am Coll Cardiol. 2011; 58:1656–1663. [PubMed: 21982309]

Mulvagh SL, DeMaria AN, Feinstein SB, Burns PN, Kaul S, Miller JG, Monaghan M, Porter TR, Shaw LJ, Villanueva FS. Contrast echocardiography: Current and future applications. J Am Soc Echocardiogr. 2000; 13:331–342. [PubMed: 10756254]

Nedelmann M, Ritschel N, Doenges S, Langheinrich AC, Acker T, Reuter P, Yeniguen M, Pukropski J, Kaps M, Mueller C, Bachmann G, Gerriets T. Combined contrast-enhanced ultrasound and rt-PA treatment is safe and improves impaired microcirculation after reperfusion of middle cerebral artery occlusion. J Cereb Blood Flow Metab. 2010; 30:1712–1720. [PubMed: 20531462]

Nishioka T, Luo H, Fishbein MC, Cercek B, Forrester JS, Kim CJ, Berglund H, Siegel RJ. Dissolution of thrombotic arterial occlusion by high intensity, low frequency ultrasound and dodecafluoropentane emulsion: An in vitro and in vivo study. J Am Coll Cardiol. 1997; 30:561–568. [PubMed: 9247533]

Phillips, PJ. Proceedings, IEEE International Ultrasonics Symposium. Vol. 2. New York: IEEE; 2001. Contrast pulse sequences (CPS): Imaging non-linear microbubbles; p. 1739-1745.

Porter TR. The utilization of ultrasound and microbubbles for therapy in acute coronary syndromes. Cardiovasc Res. 2009; 83:636–642. [PubMed: 19541670]

Porter TR, Kricsfeld D, Lof J, Everbach EC, Xie F. Effectiveness of transcranial and transthoracic ultrasound and microbubbles in dissolving intravascular thrombi. J Ultrasound Med. 2001; 20:1313–1325. quiz 1326. [PubMed: 11762543]

Porter TR, LeVeen RF, Fox R, Kricsfeld A, Xie F. Thrombolytic enhancement with perfluorocarbon-exposed sonicated dextrose albumin microbubbles. Am Heart J. 1996; 132:964–968. [PubMed: 8892768]

Postema M, van Wamel A, Lancee CT, de Jong N. Ultrasound-induced encapsulated microbubble phenomena. Ultrasound Med Biol. 2004; 30:827–840. [PubMed: 15219962]

Prasad A, Herrmann J. Myocardial infarction due to percutaneous coronary intervention. N Engl J Med. 2011; 364:453–464. [PubMed: 21288097]

Saber RS, Edwards WD, Bailey KR, Mcgovern TW, Schwartz RS, Holmes DR. Coronary embolization after balloon angioplasty or thrombolytic therapy: An autopsy study of 32 cases. J Am Coll Cardiol. 1993; 22:1283–1288. [PubMed: 8227781]

Siegel RJ, Suchkova VN, Miyamoto T, Luo H, Baggs RB, Neuman Y, Horzewski M, Suorsa V, Kobal S, Thompson T, Echt D, Francis CW. Ultrasound energy improves myocardial perfusion in the presence of coronary occlusion. J Am Coll Cardiol. 2004; 44:1454–1458. [PubMed: 15464327]

Suchkova VN, Baggs RB, Sahni SK, Francis CW. Ultrasound improves tissue perfusion in ischemic tissue through a nitric oxide dependent mechanism. Thromb Haemost. 2002; 88:865–870. [PubMed: 12428107]

Tanaka A, Imanishi T, Kitabata H, Kubo T, Takarada S, Tanimoto T, Kuroi A, Tsujioka H, Ikejima H, Komukai K, Kataiwa H, Okouchi K, Kashiwaghi M, Ishibashi K, Matsumoto H, Takemoto K, Nakamura N, Hirata K, Mizukoshi M, Akasaka T. Lipid-rich plaque and myocardial perfusion after successful stenting in patients with non-ST-segment elevation acute coronary syndrome: an optical coherence tomography study. Eur Heart J. 2009; 30:1348–1355. [PubMed: 19383736]

Topol EJ, Yadav JS. Recognition of the importance of embolization in atherosclerotic vascular disease. Circulation. 2000; 101:570–580. [PubMed: 10662756]

Villanueva FS, Gertz EW, Csikari M, Pulido G, Fisher D, Sklenar J. Detection of coronary artery stenosis with power Doppler imaging. Circulation. 2001; 103:2624–2630. [PubMed: 11382734]

Wei K, Jayaweera AR, Firoozan S, Linka A, Skyba DM, Kaul S. Quantification of myocardial blood flow with ultrasound-induced destruction of microbubbles administered as a constant venous infusion. Circulation. 1998; 97:473–483. [PubMed: 9490243]

Weller GE, Villanueva FS, Klibanov AL, Wagner WR. Modulating targeted adhesion of an ultrasound contrast agent to dysfunctional endothelium. Ann Biomed Eng. 2002; 30:1012–1019. [PubMed: 12449762]

Xie F, Lof J, Matsunaga T, Zutshi R, Porter TR. Diagnostic ultrasound combined with glycoprotein IIb/IIIa-targeted microbubbles improves micro-vascular recovery after acute coronary thrombotic occlusions. Circulation. 2009; 119:1378–1385. [PubMed: 19255341]

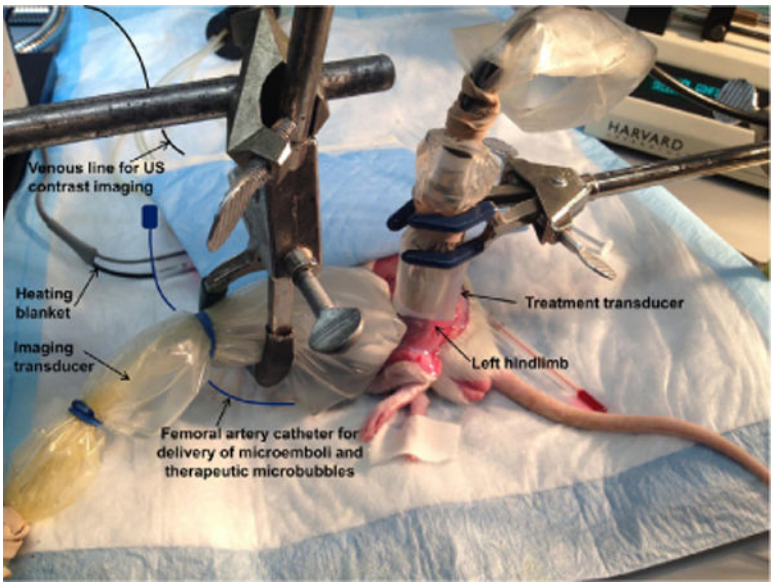

Fig. 1.
Photograph of experimental setup. US = ultrasound.

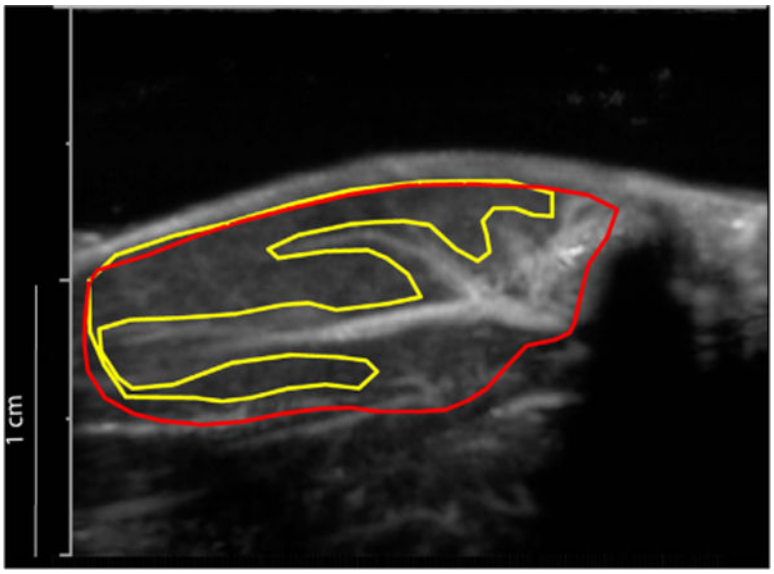

Fig. 2.

Method for selection of two regions of interest (ROIs). Frames from a movie clip were averaged into a single frame to permit distinction of the larger feeding vessels from the microcirculation (tissue perfusion, drawn in *yellow*). The *red* ROI includes both the microcirculation and larger feeding vessels.

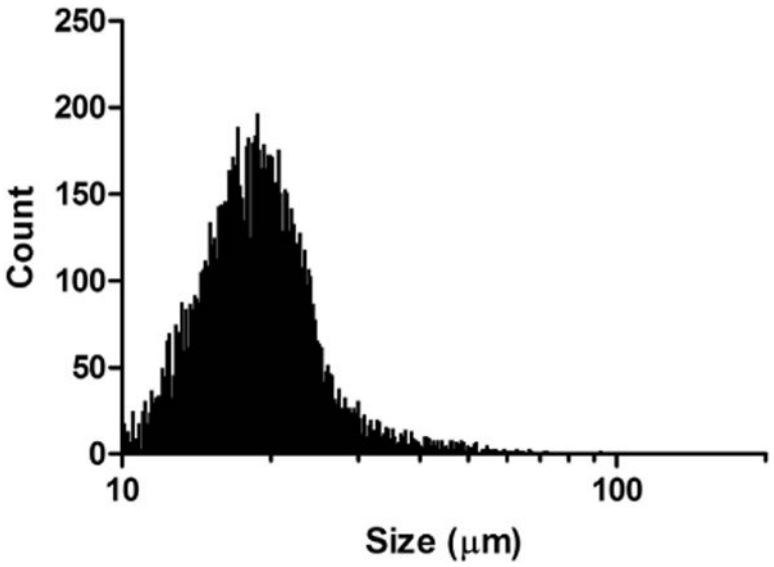

Fig. 3.

Size distribution of a representative suspension of microthrombi (total count = 10,000 particles). In this sample, particle size varied from 10 to 92.7 μm, with a mean ± standard deviation of 19.8 ± 6.8 μm.

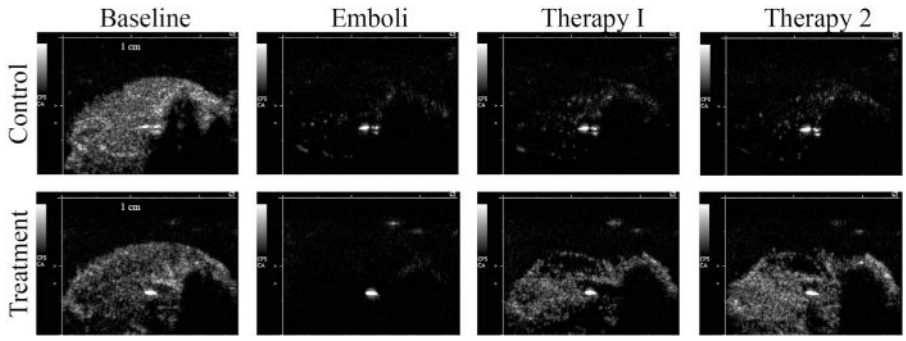

Fig. 4.

Contrast ultrasound images from representative control (top) and treatment (bottom) animals at each of four experimental stages (from left to right): baseline, embolization, therapy 1 (or control), therapy 2 (or control).

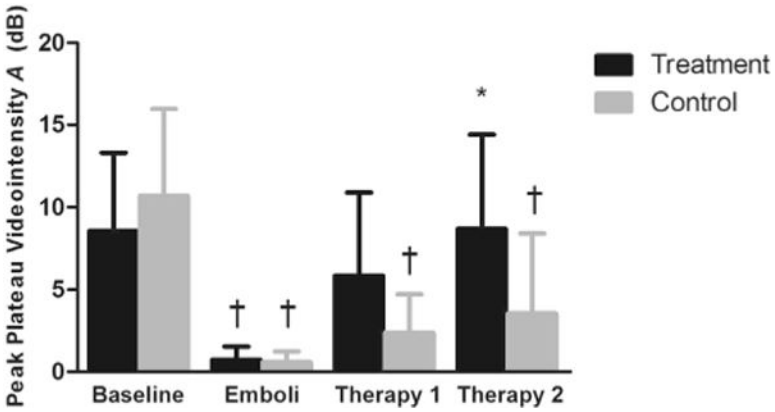

Fig. 5.

Peak plateau video intensity in the microvascular compartment. on of interest (ROI, mean ± standard deviation), reflecting microvascular cross-sectional area, at each experimental stage: Baseline; 10 min after micro-embolization (Emboli); after 10 min of ultrasound + microbubbles or no therapy (Therapy 1); and after an additional 10 min of ultrasound + microbubbles or no therapy (Therapy 2). *$p < 0.01$, compared with micro-embolization. †$p < 0.01$, compared with baseline.

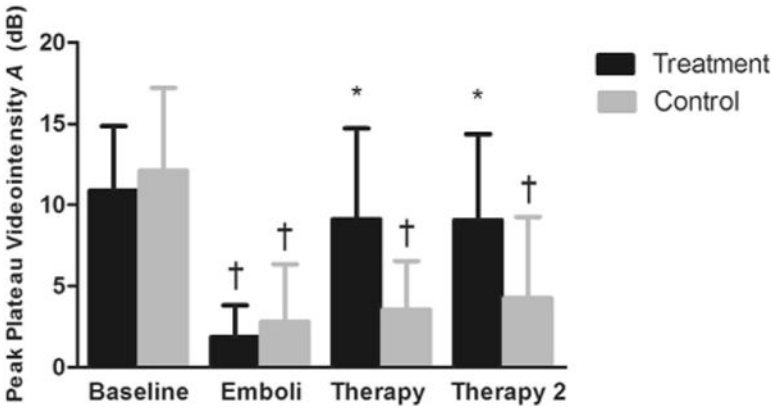

Fig. 6.

Peak plateau video intensity measured from a region of interest (ROI) drawn around the entire hindlimb muscle. ROI (mean ± standard deviation), reflecting the sum of both feeding vessel and intramuscular microvascular cross section, measured at different time points: Baseline; 10 min after micro-embolization (Emboli); 10 min after ultrasound and microbubble treatment or no treatment (Therapy 1); after an additional 10 min of ultrasound and microbubbles or no treatment (Therapy 2). *$p < 0.01$, compared with micro-embolization. †$p < 0.01$, compared with baseline.

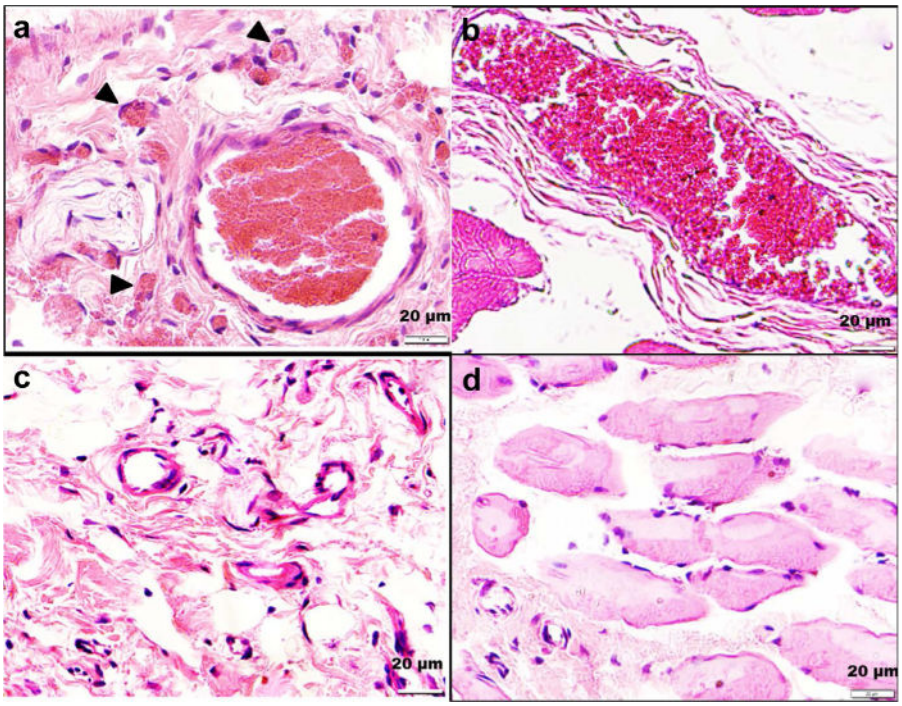

Fig. 7.

Hematoxylin and eosin-stained treated (c,d) and control (a,b) hindlimb muscle. The rats that received treatment had less microvascular obstruction than controls.